



Aerobic respiration along isopycnals leads to overestimation of the isotope effect of denitrification in the ocean water column

Dario Marconi*, Sebastian Kopf, Patrick A. Rafter, Daniel M. Sigman

Department of Geosciences, Princeton University, Princeton, NJ, USA

Received 25 April 2013; accepted in revised form 14 October 2016; available online 24 October 2016

Abstract

The nitrogen (N) isotopes provide an integrative geochemical tool for constraining the fixed N budget of the ocean. However, N isotope budgeting requires a robust estimate for the organism-scale nitrogen isotope effect of denitrification, in particular as it occurs in water column denitrification zones (ϵ_{wcd}). Ocean field data interpreted with the Rayleigh model have typically yielded estimates for ϵ_{wcd} of between 20 and 30‰. However, recent findings have raised questions about this value. In particular, culture experiments can produce a substantially lower isotope effect ($\sim 13\text{‰}$) under conditions mimicking those of ocean suboxic zones. In an effort to better understand prior field estimates of ϵ_{wcd} , we use a geochemical multi-box model to investigate the combined effects of denitrification, aerobic respiration, and isopycnal exchange on the $\delta^{15}\text{N}$ of nitrate. In the context of this admittedly simplistic model, we consider three isopycnals extending from the Southern Ocean to the Eastern Tropical North Pacific (ETNP). We show that the data from the ETNP suboxic zone can be reproduced with an ϵ_{wcd} of 13‰, given a rate of aerobic respiration consistent with the nutrient data on these isopycnals and a plausible range in the $\delta^{15}\text{N}$ of the sinking flux being remineralized. We discuss the limitations of our analysis, additional considerations, as well as possible data-based tests for the proposal of a lower ϵ_{wcd} than previously estimated. All else held constant, a lower ϵ_{wcd} would imply a lower global ocean rate of denitrification that is more similar to the estimated rate of N input to the global ocean, providing a major impetus for further investigation.

Published by Elsevier Ltd.

Keywords: Denitrification; Isotope effect; Rayleigh model

1. INTRODUCTION

Dinitrogen (N_2) is abundant in the Earth's atmosphere, but the high energy required to break its strong triple bond makes this form of N unavailable to the biosphere except through a restricted set of microorganisms capable of N fixation. Nitrogen fixing cyanobacteria in the surface waters of the open ocean appear to represent the dominant source of the ocean's bio-available ("fixed") N. Denitrification, the reduction of nitrate to N_2 (via N-oxide intermediates) during the respiration of organic matter under oxygen-deficient

conditions, represents the dominant loss of fixed N from the oceans. Denitrification occurs at significant rates both in suboxic zones of the ocean interior (water column denitrification, wcd) and in marine sediments (sedimentary denitrification, sd).

Most water column denitrification occurs in well-delineated suboxic zones in specific regions of the ocean interior (most importantly, the eastern tropical North and South Pacific and the Arabian Sea). The use of hydrographic and geochemical data allows for rate estimates for each of these denitrification zones and thus a reasonably robust global estimate for wcd (Codispoti and Christensen, 1985; Deutsch et al., 2001; DeVries et al., 2012, 2013). In contrast, sedimentary denitrification is equally or more

* Corresponding author.

E-mail address: dmarconi@princeton.edu (D. Marconi).

important on a global basis, but it is widely distributed and spatially heterogeneous, making it prohibitive to measure its globally integrated rate by direct methods. To overcome this limitation, the nitrogen isotope system has been used to constrain the partitioning between sd and wcd (Brandes and Devol, 2002). In combination with wcd rate estimates, global rates can be inferred for sd and thus for total denitrification (td, which is sd + wcd).

The partitioning between sd and wcd has been estimated as follows (Brandes and Devol, 2002): mean ocean nitrate $\delta^{15}\text{N}$ is $\sim 5\text{‰}$ vs. air and thus $\sim 6\text{‰}$ higher than that of N fixation, the main input of N to the ocean ($\delta^{15}\text{N}_{\text{IN}} \sim -1\text{‰}$; Carpenter et al., 1997). At steady state, denitrification must remove nitrate with a $\delta^{15}\text{N}$ of -1‰ (equivalent to the source). Therefore, on a global basis, the “net isotope effect” of denitrification, the isotope effect of the entire process as it applies in the environment (and in this specific case at the scale of the global ocean as a whole), is $\sim 6\text{‰}$, the positive value indicating preferential consumption of ^{14}N relative to ^{15}N (here, the isotope effect, ϵ , is defined as $1000 \left(\frac{^{14}k/^{15}k}{^{14}k/^{15}k} - 1 \right)$ in permil (‰), where ^{14}k and ^{15}k are the rate coefficients of the reactions for the ^{14}N - and ^{15}N -bearing forms of NO_3^- , respectively). This net fractionation comprises the combined fractionation from both wcd and sd, weighted for their relative rates. The isotope effect of sd, when considered at the scale of the sediment water interface, is low relative to that of wcd mostly because the nitrate flux into sediment pore waters is often consumed quantitatively, such that the biological isotope effect is not expressed outside the sediments (Brandes and Devol, 1997, 2002; Sigman et al., 2001; Sebilo et al., 2003; Lehmann et al., 2004, 2007), although nitrification can step in to cause net fractionation during N loss in some environments (Granger et al., 2011; Alkhatib et al., 2012). For simplicity, we assume that ϵ_{sd} (the net isotope effect for the entire process of sedimentary N loss at the scale of the sediment/water interface) is 0‰ . With this assumption, the partitioning between sedimentary and water column denitrification solely depends on the isotope effect of water column denitrification:

$$6\text{‰} = X_{\text{wcd}} \cdot \epsilon_{\text{wcd}} + X_{\text{sd}} \cdot \epsilon_{\text{sd}} \quad (1a)$$

$$X_{\text{wcd}} = 6\text{‰} / \epsilon_{\text{wcd}} \quad (1b)$$

$$X_{\text{sd}} = 1 - X_{\text{wcd}} \quad (1c)$$

where X_{wcd} and X_{sd} are the fractional contributions of wcd and sd to total denitrification. From (1b), the importance of the value of ϵ_{wcd} becomes apparent: the higher the isotope fractionation of wcd, the lower the wcd flux as a fraction of total ocean denitrification. Conversely, sd increases as a fraction of td. If this is combined with an independent estimate of the rate of nitrate loss by water column denitrification (e.g., DeVries et al., 2012), then a high ϵ_{wcd} implies a high td. Conversely, a smaller ϵ_{wcd} would, in turn, imply higher X_{wcd} and a lower td.

Importantly, this framework is significantly altered if one considers that water column denitrification occurs in spatially constrained suboxic zones, where it consumes a significant fraction of the nitrate locally (up to $\sim 50\%$; DeVries et al., 2013). When the global ocean exchanges

with waters from inside a suboxic zone, the $\delta^{15}\text{N}$ of the mixing product is biased towards the end member with the higher nitrate concentration, weakening the transmission of the $\delta^{15}\text{N}$ elevation to the global ocean. This dynamic, known as the “dilution effect” (Deutsch et al., 2004), is exemplified by the extreme case of sedimentary denitrification, which often consumes almost all of the nitrate at the site of denitrification (Brandes and Devol, 1997). The dilution effect leads to a weaker global isotopic impact from water column denitrification than would otherwise be the case (Deutsch et al., 2004; Eugster and Gruber, 2012; DeVries et al., 2013; Somes et al., 2013). Importantly, in our terminology from here forward, we refer to the organism-scale isotope effect for water column denitrification as ϵ_{wcd} , with the dilution effect altering the expression of this organism-level isotope effect at regional and global scales. In contrast, ϵ_{sd} refers to the isotope effect of sedimentary denitrification at the scale of the sediment/water interface, such that ϵ_{sd} subsumes the dilution effect and other biogeochemical processes in the sediments.

The primary source of quantitative constraints on ϵ_{wcd} is the analysis of nitrate isotope data from the suboxic zones, typically assuming Rayleigh distillation to represent the fractionation process in the water column. The Rayleigh model describes the isotopic evolution of a closed substrate pool as it is consumed with a constant isotope effect (Mariotti et al., 1981). Under these conditions, the nitrate $\delta^{15}\text{N}$ rises as nitrate is consumed, with $\delta^{15}\text{N}$ linearly related to the natural log of the fraction of remaining nitrate (f) with a slope of ϵ_{wcd} :

$$\delta^{15}\text{N}(\text{‰}) = \delta^{15}\text{N}_{\text{initial}} - \epsilon_{\text{wcd}} \cdot \ln(f) \quad (2)$$

Typically, f is calculated as $[\text{NO}_3^-]/(16 * [\text{PO}_4^{3-}])$ or a similar expression (Sigman et al., 2003). An inherent assumption is that all water samples derive from a single starting pair of $[\text{NO}_3^-]$ and $[\text{PO}_4^{3-}]$. The nitrate $\delta^{15}\text{N}$ and inferred values of f are often plotted in “Rayleigh space” ($\ln(f)$ on the x axis, $\delta^{15}\text{N}$ on the y axis); under the assumptions of the Rayleigh model, the slope of a regression through the data yields an estimate of the isotope effect of the consuming process. This framework is used to report results below, to facilitate comparison with expectations from the Rayleigh model.

Most estimates for ϵ_{wcd} are based on water column depth profiles through a suboxic zone, with the water below the suboxic zone taken as the assumed “initial substrate” in the Rayleigh model calculation (e.g., Brandes et al., 1998; Voss et al., 2001). This effectively assumes that deep water rises upward into the suboxic zone to undergo denitrification, with no mixing, either vertical or along isopycnals. That is, all water samples are interpreted as deep water that has undergone different degrees of denitrification and no other process. With this approach, an isotope effect of $20\text{--}30\text{‰}$ ($\sim 25\text{‰}$) is estimated for water column denitrification from ETNP data (Brandes et al., 1998; Voss et al., 2001; Sigman et al., 2003), and a similar value has been estimated from data from the Arabian Sea (Brandes et al., 1998). Altering the calculation to allow for vertical mixing (using a steady-state model) does not substantially alter the ϵ_{wcd} estimate (Brandes et al., 1998).

Such field estimates of ϵ_{wcd} were supported by the range in the isotope effect typically observed in lab culture experiments with denitrifiers (20–30‰; e.g., Barford et al., 1999). However, a recent study of denitrifiers grown under a range of growth conditions that more closely reflects the natural marine environment suggests a lower ϵ_{wcd} , closer to 13‰ (Kritee et al., 2012). Moreover, recent isopycnal analyses of data from the ETSP support the possibility of a significantly lower value for ϵ_{wcd} , with their estimates for ϵ_{wcd} falling between the two end-member possibilities of 13‰ and 25‰ considered here (Ryabenko et al., 2012; Casciotti et al., 2013).

These observations beg the question of what an ϵ_{wcd} closer to 13‰ would imply for our understanding of the marine fixed nitrogen budget. In the context of the original one-box steady state model of Brandes and Devol (2002) as well as the simple multi-box model of Deutsch et al. (2004), an ϵ_{wcd} of 25‰ yielded a low fraction of global denitrification attributed to the water column (X_{wcd} between 20% and 30%). Given estimates for the rate of water column denitrification that are unlikely to change greatly (e.g., Deutsch et al., 2001; DeVries et al., 2012), a low value for X_{wcd} implies a high total denitrification rate, substantially greater than estimates of the rate of N input (see the 25‰ scenario in Table 1). This suggestion of an imbalance only becomes worse if one considers the evidence that ϵ_{sd} is non-zero in at least some environments (Lehmann et al., 2007; Granger et al., 2011; Alkhatib et al., 2012).

More recently, inverse modeling using both a box model framework (Eugster and Gruber, 2012) and a general circulation model framework (DeVries et al., 2013) have concluded that the dilution effect allows for a much higher X_{wcd} , yielding in turn a lower global denitrification rate. These studies were a major step forward. However, the existing hydrographic data do not provide a strong constraint on where nitrate loss is occurring within the suboxic zones, a problem that is similarly encountered in porewater studies of benthic denitrification (Lehmann et al., 2007). As a result, it is a great challenge to provide a robust constraint on the global net strength of the dilution effect. Thus, we do not consider it definitive that a balanced N budget can be described with an ϵ_{wcd} of ~25‰.

In contrast, with an ϵ_{wcd} of 13‰, the calculated fixed N loss is close to being balanced with apparent N fixation rates even with the simple steady-state framework of

Brandes and Devol (2002) (Table 1). Thus, given the evidence for stability in the ocean N isotope budget over time and the evidence for negative feedbacks that should work to maintain stability in the N budget itself (Deutsch et al., 2007; Ren et al., 2009; Tyrrell, 1999; Straub et al., 2013), the “13‰ hypothesis” deserves consideration. However, as described above, an ϵ_{wcd} of 13‰ seemingly contradicts most marine estimations of ϵ_{wcd} based on Rayleigh distillation, which typically yield values of ~25‰.

Nitrite oxidation provides one potential mechanism by which the depth profile-based Rayleigh estimates may overestimate ϵ_{wcd} (Casciotti et al., 2013). It has been observed in culture that nitrite oxidation occurs with an “inverse” isotope effect, with preferential consumption of ^{15}N over ^{14}N (Casciotti, 2009). Thus, co-occurrence of nitrate reduction to nitrite and nitrite oxidation to nitrate could lead to overestimation of the isotope effect of denitrification (Casciotti et al., 2013). However, if this is the explanation, then a net ϵ_{wcd} of ~25‰ is still appropriate for ocean N isotope budgeting, as the water column N loss incorporates the isotopic impacts of any N cycling in the suboxic zones.

In this study, we investigate an alternative set of mechanisms that may lead to overestimation of isotope fractionation during water column denitrification, both the ϵ that applies at the scale of the denitrifier cell/water interface and the suboxic zone-scale value of ϵ_{wcd} to be used in N isotope budgeting. This mechanism involves the lateral circulation and oxic remineralization that occurs in the intermediate-depth ocean, along the isopycnals that ventilate the water column suboxic zones. First, the suboxic zones in which denitrification occurs are not directly sourced from the deep water underlying them but rather by circulation along isopycnals within the lower thermocline, the conditions of which are largely set in the subpolar ocean (Sarmiento et al., 2004). Second, the water outside the suboxic zones along those isopycnals contains large quantities of regenerated nitrate and phosphate from aerobic remineralization of sinking organic matter. As will be described below, this aerobic remineralization on the isopycnals that exchange with the suboxic zone may lead to substantial overestimation of ϵ_{wcd} . Here, we employ a simple model that includes the relevant process to demonstrate and investigate this potential source of bias in estimates of ϵ_{wcd} .

2. METHODS

2.1. Isotope notation

All isotopic measurements are reported in the conventional δ -notation relative to atmospheric N_2 (“air”) as the international reference:

$$\delta^{15}\text{N}(\text{‰}) = \left(\frac{(^{15}\text{N}/^{14}\text{N})_{\text{sample}}}{(^{15}\text{N}/^{14}\text{N})_{\text{air}}} - 1 \right) \cdot 1000 \quad (3)$$

Differences in the rate coefficient for reactions involving substrate bearing ^{14}N and ^{15}N (^{14}k and ^{15}k , respectively) lead to the expression of kinetic isotope effects during biochemical processes and are expressed here in ϵ -notation:

Table 1
Ocean N budget under different assumptions for ϵ_{wcd} (25‰ or 13‰). Global rates of N fixation and water column denitrification are from Gruber (2004).

ϵ_{wcd} (‰)	25	13
N fixation (Tg N/yr) ^a	135	135
wcd denitrification (Tg N/yr)	65	65
$X_{\text{wcd}}/(X_{\text{wcd}} + X_{\text{sed}})$	0.25	0.50
Sed denitrification (Tg N/yr)	205	75
Tot denitrification (Tg N/yr)	270	140
Ocean N budget (Tg N/yr)	−135	−5

^a Tg = 10^{12} g.

$$\varepsilon(\text{‰}) = ({}^{14}k/{}^{15}k - 1) \cdot 1000 \quad (4)$$

In most cases, ε is approximately the difference in $\delta^{15}\text{N}$ between the reactant and its instantaneous product (Sigman et al., 2009a).

2.2. Box model

2.2.1. Model dimensions

We selected three isopycnals in the subpolar ocean that are within the density range of waters putatively supplying the oxygen deficient zones in the ETNP as the initial water masses ($26.5 < \sigma_0 < 27.2$, where σ_0 is potential density anomaly relative to the surface; Fig. 1). Three layers of 20 boxes each are intended to represent the water along the selected isopycnals from the source (box 1) to the ETNP (box 20) (bottom panel of Fig. 2). It is important to note that the actual physical path of the water is complex. These layers are therefore not meant to represent a straight line, and the boxes' geographic locations are unconstrained.

2.2.2. Chemical constraints and mixing

The model's chemical constituents (oxygen (O_2), phosphate, and ${}^{14}\text{N}$ - and ${}^{15}\text{N}$ -nitrate) are supplied by an infinite initial reservoir (box 1 of each layer). Each of the boxes undergoes mixing exchange with its neighbors, with a certain fraction of water exchanged at each time step. For a given simulation, all mixing terms are equivalent, but the net exchange rate of box 20 with box 1 is such that box 20 has a ventilation age consistent with chlorofluorocarbon measurements (~60–80 years; Key et al., 2004).

2.2.3. Export production

Given the lateral mixing rate, the cumulative export production for the entire isopycnal is set to match observed chemical conditions in box 20, with total remineralization fueled by sinking organic matter set to match observed apparent oxygen utilization (AOU, the oxygen deficit relative to the solubility equilibrium with the atmosphere at the potential temperature and salinity of the water) and the nitrate deficit (i.e., N^*).

2.2.4. Distribution of the sinking and remineralization fluxes

To account for uncertainty in the distribution of remineralization fluxes along the isopycnals, remineralization in the model is distributed laterally across the boxes according to two different scenarios. Given the high productivity of the eastern Pacific margin, remineralization is assumed to decline away from box 20 and is modeled as a negative exponential with different cases determined by the coefficient in the exponent. In the “low focusing” scenario, remineralization decreases nearly linearly from box 20 to box 2, with only ~7% of the total export production delivered to box 20 (shaded blue area in Fig. 2a). In the “high focusing” scenario, remineralization decreases more steeply away from the suboxic box, with ~50% of the export production delivered directly to box 20 (red shaded area in Fig. 2a).

2.2.5. Stoichiometric constraints

During remineralization, ammonium in the model is released in a N:P ratio of 16:1, and, in the case of aerobic remineralization, further nitrified to nitrate. During the evaluation of the model output below, different stoichiometries are taken into consideration for the oxygen demand of remineralization (Table 2). Aerobic carbon respiration and nitrification are assumed to proceed to consume oxygen up to the point where oxygen concentration falls below the threshold values of 1.5 and 1 μM , respectively. The 1 μM oxygen concentration threshold determines the onset of denitrification (Revsbech et al., 2011).

2.2.6. Isotopic composition of the sinking and remineralized N flux

The $\delta^{15}\text{N}$ of the sinking flux (sinking $\delta^{15}\text{N}$) sets the $\delta^{15}\text{N}$ of the ammonium released by respiration from the organic matter sinking out of the surface. Nitrification of this ammonium is assumed to add nitrate to the boxes without further isotopic fractionation (i.e., the $\delta^{15}\text{N}$ of regenerated nitrate is equal to sinking $\delta^{15}\text{N}$). While there is isotope fractionation associated with the steps of nitrification, the lack of accumulation of either ammonium or nitrite in the model (and in observations; Kock et al., 2016) validates its exclusion from the model.

Given that the density of the upper isopycnal ($\sigma_0 = 26.81$) is in the density range of waters that supply nitrate to the surface, the $\delta^{15}\text{N}$ of nitrate in each box of this layer sets the upper bound for the value of the sinking $\delta^{15}\text{N}$ into that box and the boxes below it ($\sigma_0 = 26.96$ and 27.14). The rule with regard to the relationship between upper isopycnal nitrate $\delta^{15}\text{N}$ and sinking $\delta^{15}\text{N}$ was changed for different sets of simulations, with sinking $\delta^{15}\text{N}$ set to be 3–9‰ lower than the nitrate supply (see rules for sinking $\delta^{15}\text{N}$ in Table 3). As will be described below, the assumption that sinking $\delta^{15}\text{N} \leq$ nitrate supply $\delta^{15}\text{N}$ is intended to (1) take qualitative account of the effects of the partial assimilation of the surface nitrate pool and of the role of N fixation in lowering the $\delta^{15}\text{N}$ of the sinking flux (e.g., Casciotti et al., 2008), and (2) err on the side of making it difficult for our hypothesis of a low value for ε_{wed} to explain the suboxic zone nitrate $\delta^{15}\text{N}$ data.

2.2.7. Processes included in the suboxic zone

When oxygen concentration falls below a threshold of 1 μM , denitrification occurs in the model. The consequent local increase in $\delta^{15}\text{N}$ is calculated according to a constant organism-level isotope effect for water column denitrification (ε_{wed}). As described below, parallel simulations were also conducted for the $\delta^{18}\text{O}$ of nitrate ($\delta^{18}\text{O}(\text{‰}) = (({}^{18}\text{O}/{}^{16}\text{O})_{\text{sample}}/({}^{18}\text{O}/{}^{16}\text{O})_{\text{reference}} - 1) \cdot 1000$, where the reference is Vienna Standard Mean Ocean Water (VSMOW); Eq. (5)). It is assumed here that the O isotope effect of water column denitrification (${}^{18}\varepsilon_{\text{wed}}$) is equivalent in amplitude to ε_{wed} , as indicated by culture studies of denitrifiers (Granger et al., 2008).

$$\delta^{18}\text{O}(\text{‰}) = \left(\frac{({}^{18}\text{O}/{}^{16}\text{O})_{\text{sample}}}{({}^{18}\text{O}/{}^{16}\text{O})_{\text{reference}}} - 1 \right) \cdot 1000 \quad (5)$$

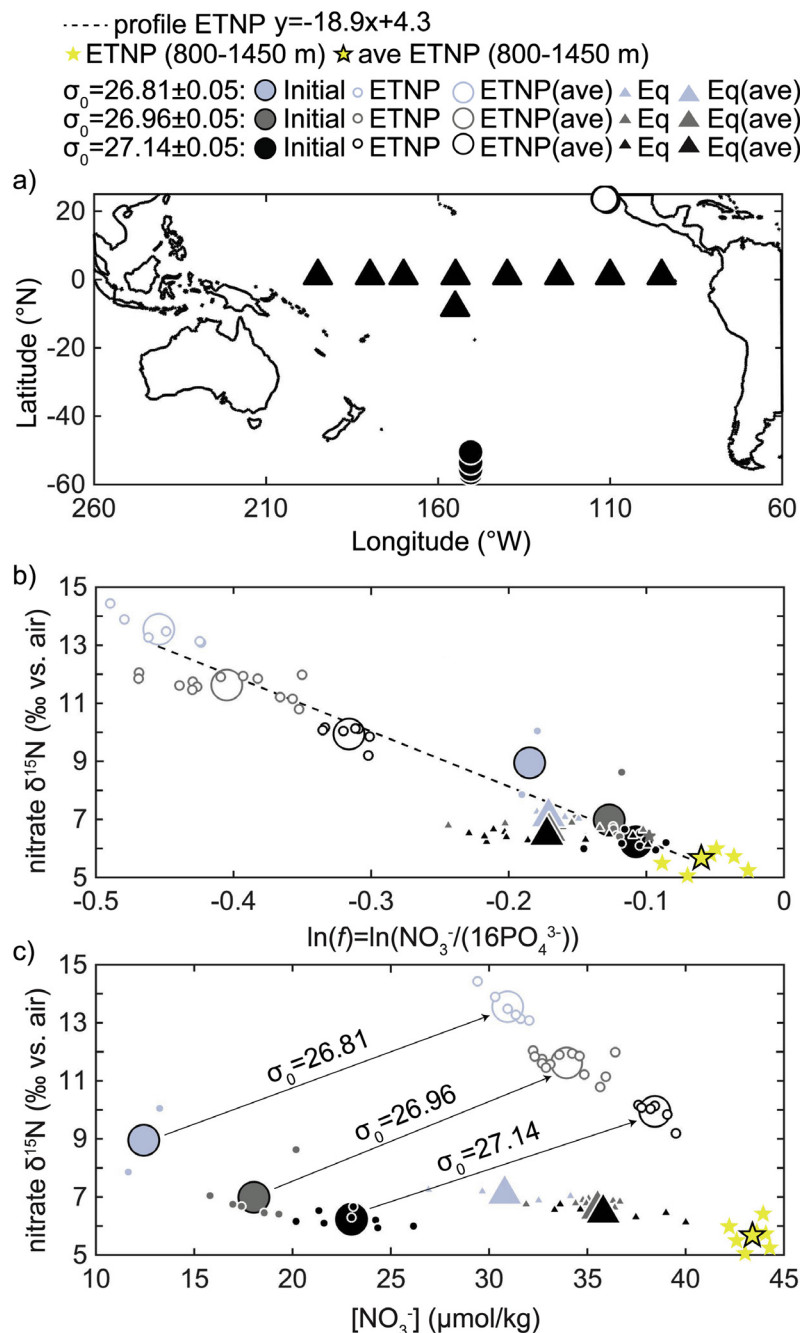


Fig. 1. Field observations used in this work. The data used to indicate the properties of the subpolar waters resupplying the three layers of the box model are labeled “Initial” (Rafter et al., 2013). Data from the Equatorial Pacific are shown as triangles and listed in the legend with the label “Eq” (Rafter et al., 2012). These data are used to compare the properties of the aerobic boxes of the model to field observations and to infer estimates for the $\delta^{15}\text{N}$ of the sinking flux. These estimates are compared to the $\delta^{15}\text{N}$ of the remineralized sinking flux used in the simulations. Data from the suboxic zone in the ETNP are shown as open circles (Sigman et al., 2005). For each of the above, small and large symbols indicate individual measurements and the average, respectively. Model output and field observations are compared along the same density intervals ($\sigma_0 = 26.81 \pm 0.05$, $\sigma_0 = 26.96 \pm 0.05$, and $\sigma_0 = 27.14 \pm 0.05$). (a) Map of sites from which the field observations derive. (b) Field observations plotted in “Rayleigh space”: nitrate $\delta^{15}\text{N}$ vs. $\ln(f)$, where $f = [\text{NO}_3^-]/16[\text{PO}_4^{3-}]$. Yellow filled stars indicate deep (800–1450 m) water in ETNP, often previously taken as the initial nitrate for “closed system” (Rayleigh model) denitrification within the suboxic zone. The dashed black line is the regression of the ETNP data only (based on the averages shown as the large yellow filled star and large open circles). The slope of this line has traditionally been interpreted as the isotope effect of water column denitrification (ϵ_{wed} ; see text). (c) $\delta^{15}\text{N}$ vs. $[\text{NO}_3^-]$ ($\mu\text{mol/kg}$) of the same field observations. The data show that nitrate concentration rises along isopycnals from high latitudes to the ETNP zone of suboxia, indicating that there is substantial aerobic remineralization of sinking N in the mid- to low latitudes. (For interpretation of the references to color in this figure legend, the reader is referred to the web version of this article.)

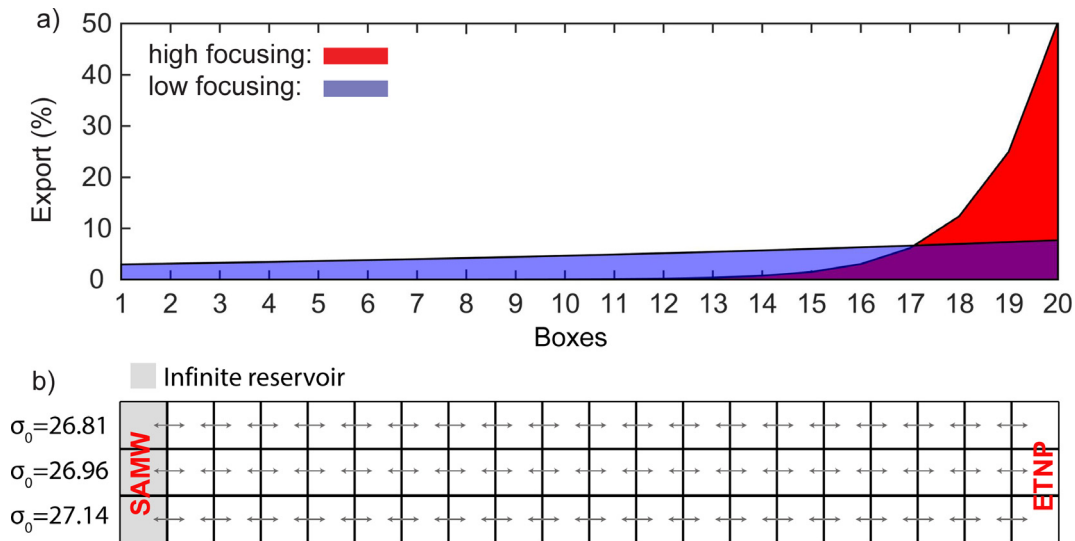


Fig. 2. Distributions of the sinking/remineralization flux (a) and isopycnal water exchange (b) in the three-isopycnal multi-box model. The three isopycnals ($\sigma_0 = 26.81 \pm 0.05$, $\sigma_0 = 26.96 \pm 0.05$, and $\sigma_0 = 27.14 \pm 0.05$) are within the density range of the Eastern Tropical North Pacific (ETNP) oxygen deficient zone ($26.5 < \sigma_0 < 27.1$). Each layer has 20 boxes. Infinite reservoirs (light grey boxes in panel b) in box 1 resupply each layer along the isopycnals; the composition of box 1 is defined by Southern Ocean data (Fig. 1; SAMW refers to Subantarctic Mode Water). The phosphate supply from the shallowest isopycnal to the surface drives the model's export production from the surface back to the isopycnals, and remineralization releases ammonium in a 16 to 1 ratio to phosphate (Table 2). The total rate of organic phosphorus regeneration on each isopycnal and its distribution between the boxes is set for each simulation according to two different cases. The high focusing case delivers 50% of the total export production to box 20. The low focusing case delivers 7% to box 20.

Table 2

Stoichiometries of aerobic respiration, nitrification and anaerobic respiration applied for the simulations (adapted from Paulmier et al., 2009). RR from Redfield et al. (1963), AN from Anderson (1995), BEC from Moore and Doney (2007).

Conditions	Nutrients released by respiration	O ₂ and NO ₃ ⁻ consumption		
		-O ₂ / PO ₄ ³⁻	-O ₂ / NH ₄ ⁺ ^a	-NO ₃ ⁻ / PO ₄ ³⁻
RR Aerobic	16	106	2	
RR Anaerobic	16			84.8
AN Aerobic	16	118	2	
AN Anaerobic	16			94.4
BEC Aerobic	16	138	2	
BEC Anaerobic	16			110.4

^a Nitrification.

Anammox (ammonium oxidation by nitrite reduction) is not explicitly included in our model. Our estimates of ε_{wcd} as well as previous estimates of ε_{wcd} by oceanic data in the context of the Rayleigh model would be impacted by any effect of anammox on the $\delta^{15}\text{N}$ of nitrate. The lack of anammox as an explicit process in our model means that the only loss mechanism for ammonium in our modeled suboxic zone (box 20) is the transport of ammonium out of box 20 by mixing. In the real ocean suboxic zones, the low levels of ammonium are probably mostly explained by consumption by anammox (Bristow et al., 2016). The poor isotopic expression typical of consumption processes that proceed to high degrees implies that including anammox and its isotope effect for ammonium oxidation (which

remains uncertain; Brunner et al., 2013) would have only minor impacts on our simulations. Other processes that result from anammox organisms, including nitrite oxidation (see below), are also not included in the model.

Nitrite oxidation has been found to represent a significant process within suboxic zones (Casciotti et al., 2013), but it is not included in our model. As described above, nitrite oxidation should work to elevate the $\delta^{15}\text{N}$ of nitrate within suboxic zones, relative to expectations from nitrate reduction alone (Casciotti et al., 2013). In this sense, the model tests the capacity of oxic remineralization along isopycnals to lead to overestimation of ε_{wcd} , but it does not address the role of nitrite oxidation, whether carried out by anammox organisms or other organisms.

2.2.8. Observational constraints for source water conditions

The subpolar ocean supplies the low latitude thermocline with preformed nutrients and oxygen by lateral exchange along isopycnals (Sarmiento et al., 2004). The oxygen supply sets the amount of aerobic remineralization occurring between the high latitude source region and the low latitude suboxic zone. The properties of the infinite reservoirs resupplying the model in the first box of each layer (grey boxes in Fig. 2b) are set by observations from the subpolar ocean (Fig. 1a, filled black circles; Fig. 1b and c, filled circles; Table 3). In spite of the geographic position of the ETNP ($\sim 20^\circ$ north of the equator), we choose SAMW (Subantarctic Mode Water) rather than NPIW (North Pacific Intermediate Water) as the ultimate source for the suboxic zone. The formation rates for SAMW are much greater than for NPIW (Hartin et al., 2011), and thus SAMW arguably represents the dominant ultimate source to tropical Pacific

Table 3

Field observations and steady state solutions of the isopycnal multi-box model. The average properties of SAMW and AAIW and the data used to supply box 1 of each isopycnal (initial) are from Rafter et al. (2013). The average properties for ETNP are from Sigman et al. (2005). The steady-state solution of the model is shown for the high and the low focusing cases, both for $\epsilon_{\text{wcd}} = 13\%$ and for $\epsilon_{\text{wcd}} = 25\%$. For each set of experiments, we show the rules for sinking $\delta^{15}\text{N}$ and the values for the apparent ϵ_{wcd} calculated as the slope of the regression of the model solution in Rayleigh space.

Water masses		σ_0 (kg/m ³)	[NO ₃ ⁻] (μmol/kg)	[PO ₄ ³⁻] (μmol/kg)	N* (μmol/kg)	[O ₂] (μmol/kg)	PO (μmol/kg)	ln(f)	NO ₃ -δ ¹⁵ N (‰ vs. air)	Sinking δ ¹⁵ N (‰)	Apparent ϵ_{wcd} (‰)							
		Mean	Mean	σ	Mean	σ	Mean	Mean	Mean	Mean	σ	Rule ^c	Mean ^d	Across ^f	Along ^e			
SAMW		26.5–27.1	21.70		1.55		-3.10		-0.13	6.3								
AAIW		27.1–27.3	30.00		2.06		-2.96		-0.09	5.8								
ETNP (800–1450 m)			44.29		3.17		-6.43		-0.13	7.0								
ETNP (200–800 m)			33.79		2.90		-12.61		-0.32	11.4								
Box 1 ^a		Mean ^b	Mean	σ	Mean	σ	Mean	Mean	Mean	σ	Mean	σ						
Layer 1 (n = 2)		26.81	12.44	1.13	0.94	0.08	-2.60	286.7	413.6	-0.18	0.01	9.0	1.6					
Layer 2 (n = 6)		26.96	18.04	1.62	1.28	0.10	-2.44	278.8	451.6	-0.13	0.01	7.0	0.8					
Layer 3 (n = 8)		27.14	22.99	1.92	1.60	0.15	-2.61	266.7	482.7	-0.11	0.02	6.2	0.3					
Box 20 (ETNP) ^a		Mean ^b	Mean	σ	Mean	σ	Mean			Mean	σ	Mean	σ					
Layer 1 (n = 6)		26.81	30.95	0.95	3.05	0.04	-17.85			-0.45	0.03	13.6	0.5					
Layer 2 (n = 13)		26.96	33.94	1.44	3.18	0.03	-16.94			-0.41	0.04	11.6	0.4					
Layer 3 (n = 7)		27.14	38.43	0.68	3.29	0.02	-14.21			-0.32	0.01	9.9	0.3					
High focusing	Specified ϵ_{wcd}	Mean ^b	Mean		Mean		Mean			Mean		Mean		Rule ^c	Mean ^d	Across ^f	B20–B1	B20–B19
Layer 1	13	26.81	31.82		3.14		-18.47			-0.46		12.9		3.8	9.2	19.4	17.7	
Layer 2	13	26.96	34.73		3.25		-17.31			-0.40		11.8		3.8	9.2		20.0	
Layer 3	13	27.14	37.62		3.25		-14.32			-0.32		10.5		3.8	9.2		23.3	
Layer 1	25	26.81	31.82		3.14		-18.47			-0.46		13.1		8.7	4.0	19.7	16.4	
Layer 2	25	26.96	34.73		3.25		-17.31			-0.40		12.1		8.7	4.0		20.0	
Layer 3	25	27.14	37.62		3.25		-14.32			-0.32		10.6		8.7	4.0		22.0	
Low focusing	Specified ϵ_{wcd}	Mean ^b	Mean		Mean		Mean			Mean		Mean		Rule ^c	Mean ^d	Across ^f	B20–B1	B20–B19
Layer 1	13	26.81	31.75		3.14		-18.43			-0.46		12.7		3.0	8.2	18.4	15.0	10.9
Layer 2	13	26.96	34.67		3.25		-17.26			-0.40		11.7		3.0	8.2		17.6	10.5
Layer 3	13	27.14	37.79		3.24		-14.07			-0.32		10.3		3.0	8.2		20.4	10.2
Layer 1	25	26.81	31.75		3.14		-18.43			-0.46		13.3		7.3	3.9	19.1	16.6	20.9
Layer 2	25	26.96	34.67		3.25		-17.26			-0.40		12.1		7.3	3.9		19.0	20.2
Layer 3	25	27.14	37.79		3.24		-14.07			-0.32		10.5		7.3	3.9		20.8	19.7

^a n is number of observations.

^b ±0.05.

^c Δδ¹⁵N (nitrate supplied-sinking PN).

^d Weighted by export fractions.

^e Slope of the ln(f) vs δ¹⁵N regression.

^f Across the three layers and starting from deep ETNP.

^g Between box 20 (B20) and box 1 (B1) or between box 20 and box 19 (B19).

thermocline waters, both north and south of the equator (Qu and Lindstrom, 2004). Moreover, adequately dense data from regions of the North Pacific that directly source the main thermocline are not yet available.

2.2.9. Observational constraints for model output

Our simulations aim to match ETNP observations for density intervals encompassing the isopycnals chosen to resupply the three layers of our model ($\sigma_0 = 26.81, 26.96, 27.14$). We compare the steady state solutions for the modeled suboxic zone (box 20 of each layer) with the ETNP measurements summarized in Table 3 (open circles in Fig. 1). An example of model output of the three-isopycnal multi-box model is shown in Fig. 3.

3. RESULTS

The model output can be compared with ocean field observations using the Rayleigh space framework. Fig. 1b shows a regression of data from a depth profile in the ETNP, which yields a slope of $\sim 19\text{‰}$ (dashed black line). Previous studies have taken such a slope as an estimate of ϵ_{wcd} , making the implicit assumption that the suboxic zone is supplied by a deep source across the isopycnals rather than by lateral exchange as in our working hypothesis (Brandes et al., 1998; Altabet et al., 1999; Voss et al., 2001; Sigman et al., 2003). The deep water source used in the regression for a vertical depth profile and our alternative subpolar thermocline water source plot in similar locations in Rayleigh space (ETNP 800–1450 m and *Initial* in Fig. 1b; Table 3). Therefore, a similar slope of $\sim 19\text{‰}$ also characterizes the

regression between the Southern Ocean and the suboxic zone in the ETNP along isopycnals. The use of the Southern Ocean subpolar thermocline as the nitrate source therefore does not change the ϵ_{wcd} estimate in the narrow context of the Rayleigh space visualization (Fig. 1b). However, it implies substantially lower nitrate concentration of the source waters, which must become elevated by aerobic remineralization of the sinking flux along isopycnals *en route* to the suboxic zone (Fig. 1c). In the next sections, we present our findings from box model simulations with the two different scenarios for the distribution of sinking flux remineralization described above (“7% focusing” and “50% focusing”). For both cases, we run simulations under two different assumptions for $\epsilon_{\text{wcd}} = 13\text{‰}$ and 25‰ – and identify the boundary conditions required to match observations.

3.1. Fitting nutrient observations in the model’s suboxic box

The experiments are aimed to match nutrient observations in the ETNP suboxic zone (NO_3^- , PO_4^{3-} and thus also N^* , defined here as $\text{NO}_3^- - 16\text{PO}_4^{3-}$). Similar matches are achieved for both high and low focusing scenarios. In both cases, a match to ETNP observations starting from SAMW waters requires different stoichiometries for the remineralized material on the different isopycnals (Supplementary Fig. 1). These results are consistent with an increase with depth in the O_2 consumption per phosphate remineralized from the shallowest to the deepest isopycnals (from σ_0 of 26.81–27.14) that has been observed previously (Paulmier et al., 2009). Here we model this increase as ranging from a Redfieldian O_2 -to- PO_4^{3-} ratio of 106:1 in the shallowest

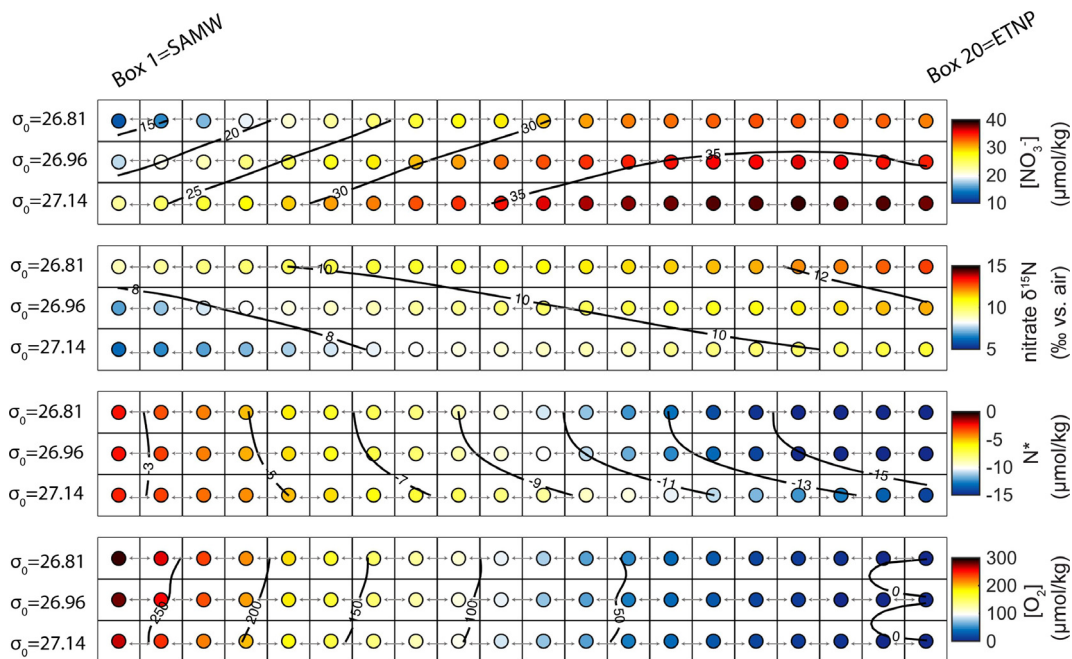


Fig. 3. Example of model output from the three-isopycnal multi-box model, showing the low focusing case and a specified ϵ_{wcd} of 13‰ . Modeled $[\text{NO}_3^-]$, nitrate $\delta^{15}\text{N}$, N^* and $[\text{O}_2]$ are shown for the 20 boxes of each isopycnal. In each box, the $\delta^{15}\text{N}$ of the sinking flux is a function of the $\delta^{15}\text{N}$ of the nitrate supply to the overlying surface at the location of that box. Specifically, the $\delta^{15}\text{N}$ of the sinking flux is lower than the $\delta^{15}\text{N}$ of the nitrate supply by an amount given in Table 3. Anaerobic conditions are encountered in box 20 of each layer. Denitrification in box 20 occurs with constant ϵ_{wcd} (25‰ or 13‰). Uniform lateral mixing occurs along the isopycnals (arrows between boxes).

isopycnal to the 138:1 in the deepest isopycnal as estimated previously using an ocean model with biogeochemical cycling (RR and BEC in Table 2; Redfield et al., 1963; Moore and Doney, 2007). The downward increase in O_2 consumption reflects the higher aerobic remineralization potential of the deeper isopycnals, as quantified by the conservative tracer PO ($135 * PO_4^{3-} + O_2$) that captures both realized and potential nutrient remineralization (Table 3).

3.2. Fitting nitrate $\delta^{15}N$ in the model's suboxic box

The simulations aiming to reproduce the suboxic zone from a SAMW source achieve a comparable match to the ETNP nitrate $\delta^{15}N$ data for both the high and the low focusing scenarios (Fig. 4). Nitrate $\delta^{15}N$ in the ETNP can be made to match observations with either the canonical ϵ_{wcd} of 25‰ or the lower ϵ_{wcd} of 13‰ by allowing the $\delta^{15}N$ of the sinking N-derived, remineralized nitrate flux into the isopycnals to vary (Fig. 5). A cost-minimization function comparing the model output at steady-state to the observations for the three layers of the model was used to find the best fit values for the $\delta^{15}N$ of the sinking N (Wald, 1949; Nikulin, 2001).

For the simulations assuming $\epsilon_{wcd} = 25‰$, matching the ETNP observations implies a weak decoupling between the ϵ_{wcd} specified for the simulations and the resulting slope of the regression in Rayleigh space. For both the high and the low focusing scenarios, the apparent isotope effect as given by the slope of the Rayleigh regression between box 1 (Southern Ocean) and box 20 (modeled ETNP) in each layer ranges between 16.4 and 22.0‰ (Fig. 6a). Therefore, the apparent isotope effect underestimates the true ϵ_{wcd} of 25‰ specified in the simulations by 3.0 to 8.6‰.

Conversely, matching the ETNP observations with an ϵ_{wcd} of 13‰ requires a strong amplification of the $\delta^{15}N$ elevation due to denitrification. The data fitting protocol results in regression slopes between 17.7 and 23.3‰ for the high focusing scenario and between 15.0 and 20.4‰ for the low focusing scenario, yielding an overestimation

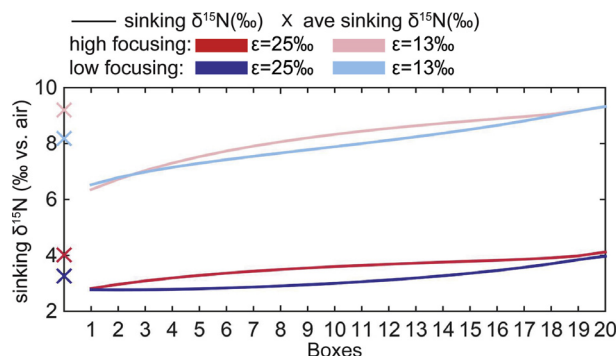


Fig. 5. Lateral distribution of the $\delta^{15}N$ of the sinking flux across the model domain. Solid lines indicate individual values for each box of the isopycnal model, while crosses on the left side of the panel display the isopycnal averages. The high and low focusing cases are shown in red and blue, respectively (Table 3). (For interpretation of the references to color in this figure legend, the reader is referred to the web version of this article.)

of the specified ϵ_{wcd} (13‰) by 4.7–10.3‰ for the high focusing case and by 2.0–7.4‰ for the low focusing case (Fig. 6a).

In all cases, two main processes are at work. The first is the “mixing effect”, which derives from mixing suboxic waters that have undergone partial nitrate consumption with oxic waters of the open ocean; this is the regional-scale counterpart to the global scale “dilution effect” described above (Deutsch et al., 2004). The second process is the aerobic remineralization of the sinking flux. The mixing effect always pushes the apparent isotope effect below the true ϵ_{wcd} . Aerobic remineralization of the sinking flux can lead to over- or under-estimation of ϵ_{wcd} , depending on the $\delta^{15}N$ of the sinking flux. The over-estimation of the isotope effect required in simulations with a low ϵ_{wcd} of 13‰ implies that mixing effects are countered by a high sinking $\delta^{15}N$ of 9.2‰ (Fig. 5b; Table 3). Conversely, the under-estimation required to match ETNP observations

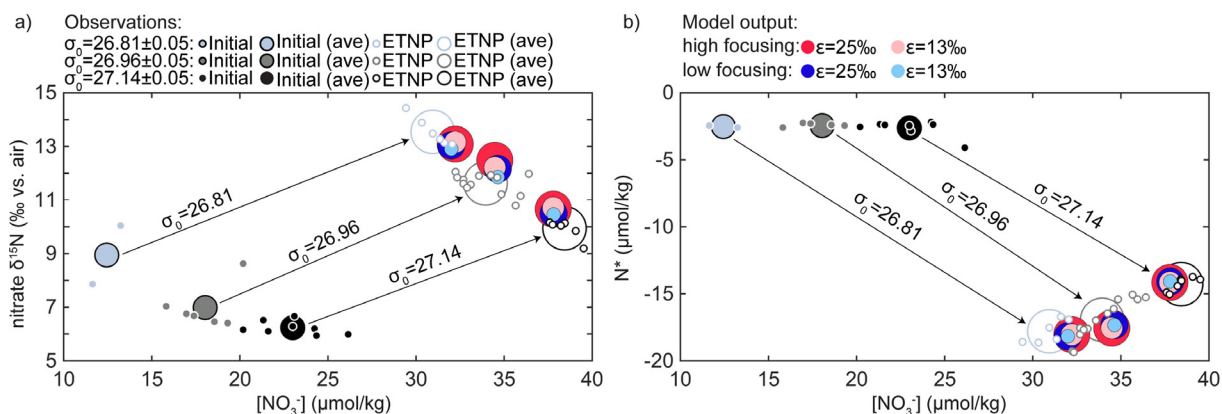


Fig. 4. Comparison of the model solutions with field observations. The model output is compared with the Southern Ocean and ETNP observations along the three isopycnal layers of the model for the high focusing case (dark red for a specified ϵ_{wcd} of 25‰ and light red for a specified ϵ_{wcd} of 13‰; Table 3) and the low focusing case (dark blue for a specified ϵ_{wcd} of 25‰ and light blue for a specified ϵ_{wcd} of 13‰; Table 3). (a) Comparison in $\delta^{15}N$ vs. $[NO_3^-]$ space. (b) Comparison in N^* vs. $[NO_3^-]$ space. (For interpretation of the references to color in this figure legend, the reader is referred to the web version of this article.)

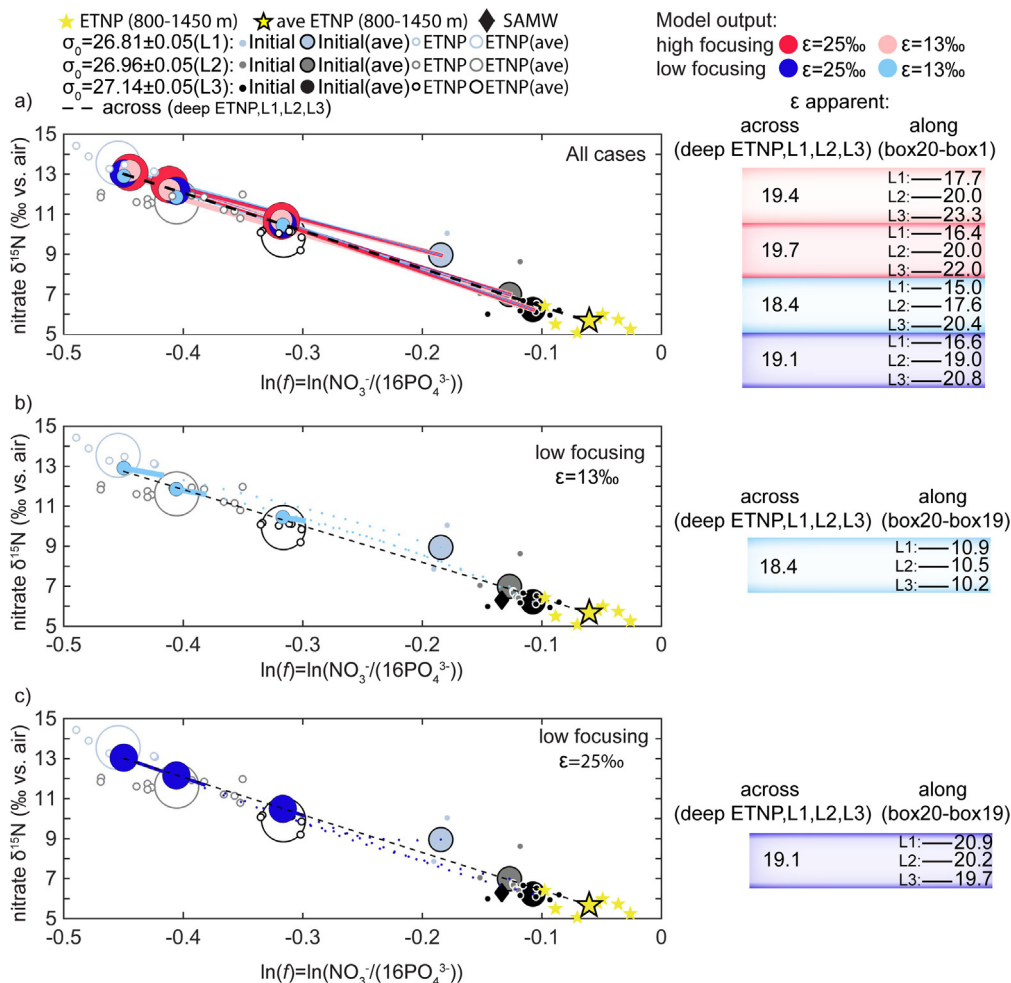


Fig. 6. Comparison of the ϵ_{wcd} specified for the simulations and the apparent ϵ_{wcd} calculated from the model solutions. The apparent ϵ_{wcd} is calculated as the slope of the regression of the model solutions in Rayleigh space ($\delta^{15}\text{N}$ vs. $\ln(f)$). (a) For the four cases of this work (high and low focusing scenarios; ϵ_{wcd} of 13‰ and ϵ_{wcd} of 25‰), apparent ϵ_{wcd} is calculated for a hypothetical depth profile in the model running from the deep ETNP (yellow filled star) through the three layers of box 20 in the model (“across”; Table 3) and along isopycnals between box 20 and box 1 for each layer (“along”; Table 3). (b, c) For the low focusing cases, apparent ϵ_{wcd} is calculated for the same hypothetical depth profile as in (a) (“across”; Table 3) and isopycnally between box 20 and box 19 of each layer (“along”; Table 3). (For interpretation of the references to color in this figure legend, the reader is referred to the web version of this article.)

with an ϵ_{wcd} of 25‰ implies that mixing effects are compounded by a low average $\delta^{15}\text{N}$ of the sinking flux of $\sim 4\text{‰}$ (Fig. 5b; Table 3). Accordingly, information on the $\delta^{15}\text{N}$ of sinking material across the Pacific, weighted for sinking and remineralization rate, is crucial to determine whether the true ϵ_{wcd} is lower than has so far been estimated from water column data. Below, we explore these implications with sensitivity tests of our isopycnal model (Table 4).

4. INTERPRETATION

4.1. The effect of aerobic respiration in Rayleigh space

To evaluate the distorting effects of remineralized sinking material on linear regressions in Rayleigh space, and consequently on the apparent isotope effect derived from them, it is insightful to start by considering the case of sinking material that does not have an impact on the ϵ_{wcd} estimated with the Rayleigh model (here termed the “sinking

limit”). In the case of “Redfieldian” organic matter (i.e. with a N/P of 16, Table 2), the addition of nutrients by aerobic remineralization does not change the nitrate deficit N^* , but it does change the fraction of nitrate remaining from denitrification, the parameter f in Eq. (2). The parameter f is calculated as $[\text{NO}_3^-]/([\text{NO}_3^-] - N^*)$, equivalent to $[\text{NO}_3^-]/16[\text{PO}_4^{3-}]$. Here, we define “ $\ln(f_{\text{gain}})$ ” as the change in the natural log of f caused by the addition of regenerated nutrients and expressed as a function of the nutrient concentrations before aerobic respiration (N_{bae} and P_{bae}) and the concentration of phosphate added by the remineralization of sinking organic matter (P_{sink} ; see Supplementary Fig. 2):

$$\ln(f_{\text{gain}}) = \ln \left[\left(\frac{N_{\text{bae}}}{N_{\text{bae}} + 16 \cdot P_{\text{sink}}} \right) \cdot \left(\frac{P_{\text{bae}} + P_{\text{sink}}}{P_{\text{bae}}} \right) \right] \quad (6a)$$

The effect of aerobic respiration on the slope of the trend in Rayleigh space (i.e. the apparent isotope effect) depends on this change in $\ln(f)$. An increase in $\ln(f)$ would cause an

Table 4

Sensitivity test conducted along the shallowest isopycnal of the model ($\sigma_0 = 26.81$). A sinking $\delta^{15}\text{N}$ progressively greater than sinking $\delta^{15}\text{N}_{\text{limit}}$ causes the apparent ϵ_{wcd} , calculated from the model solutions, to deviate from the ϵ_{wcd} specified for the simulations.

Sensitivity test	Specified ϵ_{wcd}	σ_0 (kg/m^3)	$[\text{NO}_3^-]$ ($\mu\text{mol/kg}$)	$[\text{PO}_4^{3-}]$ ($\mu\text{mol/kg}$)	$\ln(f)$	NO_3^- - $\delta^{15}\text{N}$ (‰)	Sinking $\delta^{15}\text{N}$ (‰)	Apparent ϵ_{wcd} ^a (‰)
High focusing								
Layer 1	13	26.81 ± 0.05	31.82	3.14	-0.46	11.0	Sinking $\delta^{15}\text{N}_{\text{limit}}$	Along ^b
	13	26.96 ± 0.05	34.73	3.25	-0.40	12.5	Sinking $\delta^{15}\text{N}_{\text{limit}} + 2$	7.5
	13	27.14 ± 0.05	37.62	3.25	-0.32	13.9	Sinking $\delta^{15}\text{N}_{\text{limit}} + 4$	13.8
Low focusing								
Layer 1	13	26.81 ± 0.05	31.75	3.14	-0.46	11.4	Sinking $\delta^{15}\text{N}_{\text{limit}}$	Along ^b
	13	26.96 ± 0.05	34.67	3.25	-0.40	12.8	Sinking $\delta^{15}\text{N}_{\text{limit}} + 2$	8.1
	13	27.14 ± 0.05	37.79	3.24	-0.32	14.3	Sinking $\delta^{15}\text{N}_{\text{limit}} + 4$	13.6
								19.1

^a Slope of the $\ln(f)$ vs $\delta^{15}\text{N}$ regression.

^b Between all 20 boxes.

increase in the slope of the regression between the *initial* and the denitrified nitrate pool (Fig. 7). This effect on the slope can be counterbalanced by the change in the $\delta^{15}\text{N}$ of nitrate if the added (regenerated) nitrate has a $\delta^{15}\text{N}$ that is adequately low. We define $\delta^{15}\text{N}_{\text{bae}}$ as the $\delta^{15}\text{N}$ of nitrate before the addition of regenerated nutrients and use the concept of $\ln(f_{\text{gain}})$ to set the above-mentioned Rayleigh-neutral threshold value for the $\delta^{15}\text{N}$ of the nitrate added by remineralization of the sinking flux, the “sinking limit”, sinking $\delta^{15}\text{N}_{\text{limit}}$ (see Supplementary Fig. 2):

$$\text{sinking } \delta^{15}\text{N}_{\text{limit}} = \delta^{15}\text{N}_{\text{bae}} + \epsilon \cdot \ln(f_{\text{-gain}}) + \left[\epsilon \cdot \ln(f_{\text{-gain}}) \cdot \frac{\text{N}_{\text{bae}}}{(16 \cdot \text{P}_{\text{sink}})} \right] \quad (6b)$$

If sinking $\delta^{15}\text{N}$ is equal to sinking $\delta^{15}\text{N}_{\text{limit}}$, the decrease in the $\delta^{15}\text{N}$ of the nitrate pool balances the increase in $\ln(f)$ ($\ln(f_{\text{gain}})$) and therefore aerobic respiration has no effect on the slope of the Rayleigh regression (Fig. 7). If sinking $\delta^{15}\text{N}$ is greater than sinking $\delta^{15}\text{N}_{\text{limit}}$, the change in $\ln(f)$ ($\ln(f_{\text{gain}})$) is greater than the decrease in the $\delta^{15}\text{N}$ of the nitrate pool. The change in $\ln(f)$ pulls the water parcel to the right and above the Rayleigh substrate trend hence yielding an *apparent* ϵ_{wcd} that is greater than the *true* ϵ_{wcd} (Fig. 7).

4.2. Sensitivity test of sinking $\delta^{15}\text{N}$

We apply the concept of sinking $\delta^{15}\text{N}_{\text{limit}}$ to quantify the potential of the sinking flux to modulate the effect of aerobic respiration on the slope of the Rayleigh regression along an isopycnal ($\sigma_0 = 26.81$). In these model simulations, sinking $\delta^{15}\text{N}$ is prescribed and (nearly) constant across the boxes, in contrast to the fixed relationship with the $\delta^{15}\text{N}$ of nitrate in each of the boxes of the shallow isopycnal that was used in the data fitting exercise (Section 3). For both the high and low focusing scenarios, simulations with sinking $\delta^{15}\text{N}$ equal to sinking $\delta^{15}\text{N}_{\text{limit}}$ add remineralized material along the isopycnals that is isotope effect-neutral (Fig. 8, open squares). Therefore, only the mixing effect works to obscure the true ϵ_{wcd} . In this case, the resulting apparent ϵ_{wcd} is $\sim 8\text{‰}$, under-estimating the true ϵ_{wcd} (13‰) by $\sim 5\text{‰}$ (“ ϵ apparent” in Fig. 8b).

The experiments run with a sinking $\delta^{15}\text{N}$ greater than sinking $\delta^{15}\text{N}_{\text{limit}}$ yield higher apparent ϵ_{wcd} (open triangles and small open circles in Fig. 8). The extent of ϵ_{wcd} over-estimation depends on the difference between sinking $\delta^{15}\text{N}$ and sinking $\delta^{15}\text{N}_{\text{limit}}$. A 2‰ difference balances the under-expression caused by the mixing effect and results in an apparent ϵ_{wcd} of 13‰ (open triangles in Fig. 8), while a greater difference yields over-estimation of ϵ_{wcd} in Rayleigh space. If sinking $\delta^{15}\text{N}$ is 4‰ greater than sinking $\delta^{15}\text{N}_{\text{limit}}$, the modeled suboxic zone (box 20) matches ETNP observations, yielding an apparent isotope effect of $\sim 20\text{‰}$ for the high focusing case and $\sim 19\text{‰}$ for the low focusing case (small open circles in Fig. 8).

4.3. Potential observational constraints

The calculations described above suggest that ETNP data may be reproduced from known source waters in the Southern Ocean under different assumptions for ϵ_{wcd} (25‰ or 13‰). The “ 25‰ ” simulations require a weak impact of aerobic respiration on the slope of the Rayleigh regression along the isopycnals. Conversely, the “ 13‰ ” simulations call for a major role for aerobic respiration in raising the slope. For a given ratio of regenerated to pre-formed nutrients on a given isopycnal, the strength of the distorting effect of aerobic respiration ultimately depends on the difference between sinking $\delta^{15}\text{N}$ and sinking $\delta^{15}\text{N}_{\text{limit}}$ (Fig. 8).

For these reasons, the 25‰ and the 13‰ scenarios, both adjusted to fit observations, differ substantially in their predictions of the $\delta^{15}\text{N}$ of sinking N (sinking $\delta^{15}\text{N}$) that is consistent with suboxic zone nitrate $\delta^{15}\text{N}$ data. If the true ϵ_{wcd} is 25‰ , an average sinking $\delta^{15}\text{N}$ of $\sim 4.0\text{‰}$ and $\sim 3.9\text{‰}$ is required for the high and the low focusing scenarios, respectively (Table 3). A true ϵ_{wcd} of 13‰ would imply a higher average sinking $\delta^{15}\text{N}$ of $\sim 9.2\text{‰}$ or $\sim 8.1\text{‰}$ (high and low focusing scenarios, in Table 3). Assuming an approximately linear relationship between ϵ_{wcd} and the mean sinking $\delta^{15}\text{N}$ required to match ETNP observations, our modeling results suggest that the true ϵ_{wcd} in the ocean could be estimated from data on the $\delta^{15}\text{N}$ of sinking N if adequately extensive data sets were available (Fig. 9a).

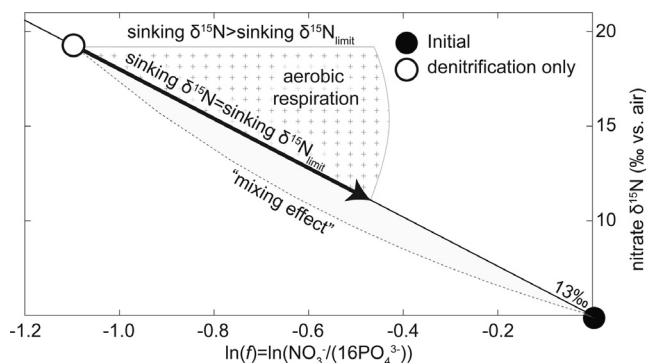


Fig. 7. Effect of aerobic remineralization in Rayleigh space. Sinking $\delta^{15}\text{N}_{\text{limit}}$ is a threshold value for the $\delta^{15}\text{N}$ of sinking N. If sinking $\delta^{15}\text{N}$ equals sinking $\delta^{15}\text{N}_{\text{limit}}$, a mixture of the denitrified nitrate pool and the nitrate added by aerobic respiration causes no deviation from the line with a slope of true ϵ_{wcd} (which is specified at 13‰ in the example shown). The arrow indicates the effect of aerobic remineralization if sinking $\delta^{15}\text{N}$ equals sinking $\delta^{15}\text{N}_{\text{limit}}$. If sinking $\delta^{15}\text{N}$ is greater than sinking $\delta^{15}\text{N}_{\text{limit}}$, the mixing product plots above the 13‰ line (stippled area; see also [Supplementary Fig. 2](#)). To indicate the qualitative effect of mixing in Rayleigh space, the mixing curve between the source (filled circle) and partially denitrified water (open circle) is shown with a dotted line.

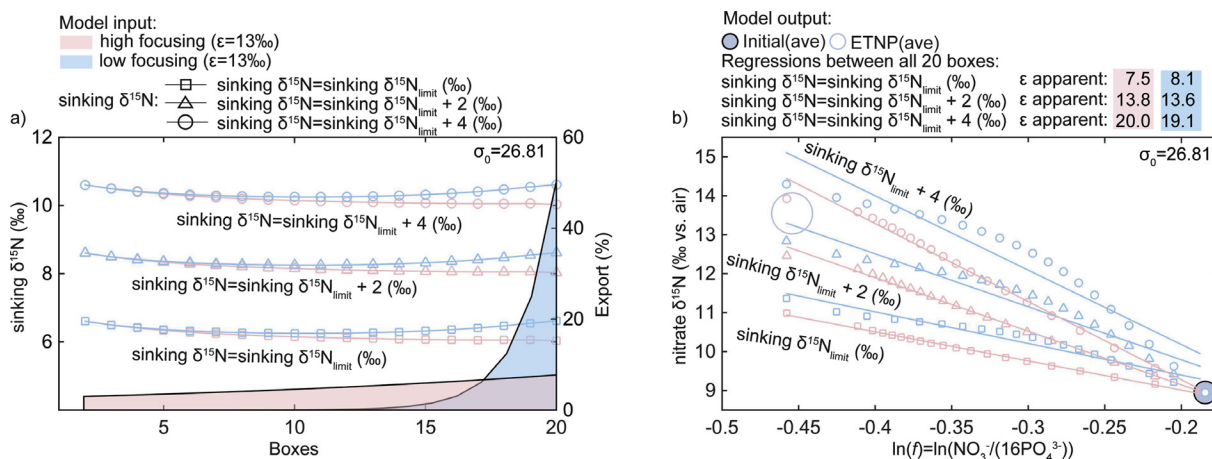


Fig. 8. Sensitivity tests of the model output to sinking $\delta^{15}\text{N}$. The tests are conducted in the shallowest isopycnal of the model ($\sigma_0 = 26.81 \pm 0.05$) for the high and low focusing cases (with $\epsilon_{\text{wcd}} = 13\text{‰}$) (see equations in [Supplementary Fig. 2](#)). (a) Distribution of the remineralization/sinking flux and $\delta^{15}\text{N}$ of the sinking flux for each box of the layer. (b) Results of the sensitivity test in Rayleigh space and apparent ϵ_{wcd} calculated as the slope of the regression of the model solutions (along the 20 boxes of the layer). Increasing sinking $\delta^{15}\text{N}$ above sinking $\delta^{15}\text{N}_{\text{limit}}$ drives an increase in the slope of the regression in Rayleigh space, so that the apparent ϵ_{wcd} is greater than the value of ϵ_{wcd} specified for the simulations ([Table 4](#)).

There are mechanistic prerequisites for sinking flux $\delta^{15}\text{N}$ to possibly be as high as $\sim 9\text{‰}$ ($\epsilon_{\text{wcd}} = 13\text{‰}$) or as low as 4‰ ($\epsilon_{\text{wcd}} = 25\text{‰}$). The former requires that fixed N with high $\delta^{15}\text{N}$ that is generated in the eastern Pacific denitrification zones is transported into surrounding oxic waters to a substantial degree, by a combination of physical nitrate transport and biological N cycling ([Sigman et al., 2009c](#)). The latter requires N inputs with low $\delta^{15}\text{N}$ from N fixation ([Casciotti et al., 2008](#)). As both processes are known to occur, it seems most appropriate to take an empirical approach to constrain the average value of the sinking flux $\delta^{15}\text{N}$ across the regions that would contribute regenerated N to our isopycnals of interest.

Unfortunately, the available sediment trap $\delta^{15}\text{N}$ data are not adequate to clearly support either of the $\delta^{15}\text{N}$ ranges required to match ϵ_{wcd} of 13 or 25‰ ([Robinson](#)

[et al., 2012](#)), in part because many of the sediment trap deployments have been focused on the isotope dynamics of progressive nitrate consumption by assimilation in nutrient-rich surface waters, leading to broad ranges in the measured $\delta^{15}\text{N}$ of sinking N (e.g., [Altabet and Francois, 1994](#)). Instead, we use estimates of the $\delta^{15}\text{N}$ of sinking N inferred from the change in the $\delta^{15}\text{N}$ of nitrate in equatorial waters (black triangles in [Fig. 1](#)) relative to their source in the Southern Ocean (black circles in [Fig. 1](#)). The fraction of total phosphate that is regenerated ($P_{\text{reg}}/P_{\text{tot}}$) provides a metric to track the extent of remineralization ([Sigman et al., 2009b](#); [Rafta et al., 2013](#); [Marconi et al., 2015](#)). P_{reg} is assumed to equal $\text{AOU} * (1/150)$. The relationship between the $\delta^{15}\text{N}$ of nitrate and the $P_{\text{reg}}/P_{\text{tot}}$ ratio can be extrapolated to provide an estimate for the $\delta^{15}\text{N}$ of regenerated nitrate and thus for the $\delta^{15}\text{N}$ of sinking

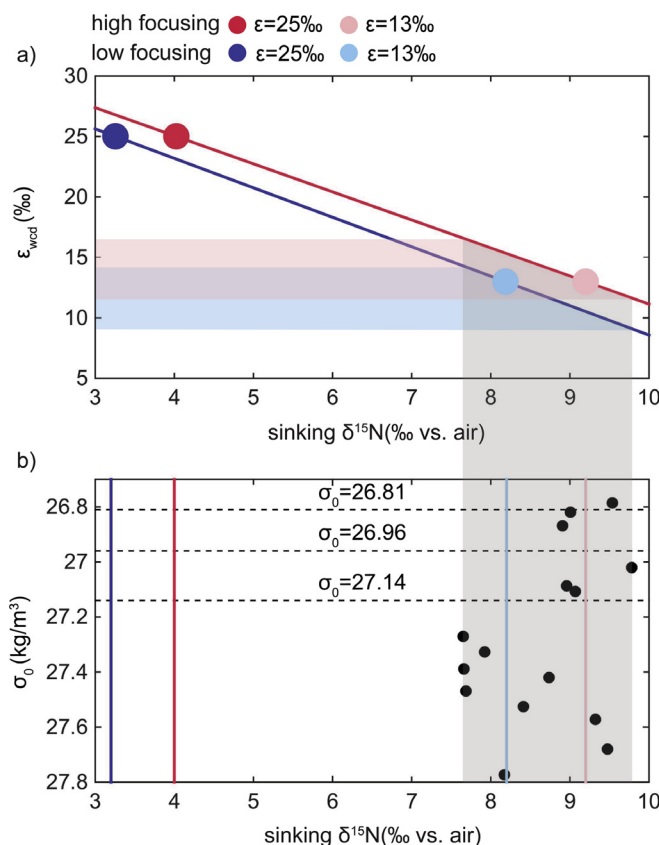


Fig. 9. The ocean's value for ϵ_{wcd} as suggested by field-based estimates of the $\delta^{15}N$ of sinking N. (a) Filled circles summarize the results of the experiments for the four cases of this study. The high focusing case for aerobic remineralization is shown in dark red for ϵ_{wcd} of 25‰ and light red for ϵ_{wcd} of 13‰. The low focusing case is shown in dark blue for ϵ_{wcd} of 25‰ and light blue for ϵ_{wcd} of 13‰. Assuming a linear relationship between ϵ_{wcd} and the mean sinking $\delta^{15}N$ required to match ETNP observations (red line for the high focusing case and blue line for the low focusing case), true ϵ_{wcd} in the ocean can be estimated from data on the $\delta^{15}N$ of sinking N. (b) Estimates of sinking N $\delta^{15}N$ from field observations (black circles; see [Supplementary Fig. 3](#)) are compared to values of sinking $\delta^{15}N$ required for our simulations to match field observations of nitrate $\delta^{15}N$ (vertical colored lines projected from filled circles in panel a to panel b). The high $\delta^{15}N$ of sinking N from field observations (ranging between 7.6 and 9.8‰) is consistent with an ϵ_{wcd} much lower than 25‰. The projection of the range of observations (grey shaded area) from panel b to panel a is used to display our best estimate for the true ϵ_{wcd} . Light red shaded area displays the range of the estimate for the true ϵ_{wcd} for the high focusing case. Light blue shaded area indicates the range for the low focusing case. The overlap between the estimates from the high and low focusing cases is shown as the overlap region of red and blue shadings in (a). (For interpretation of the references to color in this figure legend, the reader is referred to the web version of this article.)

N ([Supplementary Fig. 3](#)). We use P_{reg}/P_{tot} instead of a nitrate-based metric because the latter would be affected by N fixation or denitrification. This analysis suggests that the regenerated nitrate added to SAMW between its formation region and the equatorial region has a $\delta^{15}N$ between 7.6 and 9.8‰ for the density range of our model ([Fig. 9b](#)). Based on a similar approach, an estimate of 9.0‰ was derived from South Pacific data by [Raftter et al. \(2013\)](#). These estimates point to a sinking $\delta^{15}N$ that would allow an ϵ_{wcd} of 13‰ to explain the data from the ETNP suboxic zone ([Fig. 9b](#)). Further support for this result is provided by the fact that nitrate with a still higher $\delta^{15}N$ is likely added closer to the suboxic zones.

A second set of potential observational constraints for distinguishing between high and low ϵ_{wcd} involves nitrate $\delta^{15}N$ in the waters adjacent to the suboxic zones. The model suggests aerobic respiration as a mechanism to obscure the true value of ϵ_{wcd} . However, substantial nitrate

regeneration probably does not occur within the suboxic zones themselves. Therefore, the slope of the Rayleigh regression between the suboxic zone (box 20) and the adjacent aerobic waters along the isopycnals (box 19, here assumed as the nitrate source for the suboxic zone) cannot exceed that imposed by ϵ_{wcd} . Indeed, some underestimation of ϵ_{wcd} is expected due to the mixing effect. This dynamic appears in our simulations ([Fig. 6b](#) and [c](#)). Thus, as one approaches the suboxic zone, the nitrate isotope changes along isopycnals should more accurately capture the true ϵ_{wcd} . [Ryabenko et al. \(2012\)](#) carry out such an analysis in the ETSP. Remarkably, their data imply a relatively low ϵ_{wcd} of 16.0‰, although the authors attribute this low value to the influence of benthic denitrification at the margin. Also in the ETSP, [Casciotti et al. \(2013\)](#) carry out an analysis along three isopycnal ranges, yielding ϵ_{wcd} estimates between 15.7‰ (on shallower isopycnals) and 21.5‰ (on deeper isopycnals).

A third observational approach is to use the decrease in N_2 $\delta^{15}N$ observed in the core of the suboxic zone to infer the $\delta^{15}N$ of the N_2 excess produced by the denitrification of nitrate (Brandes et al., 1998; Kononov et al., 2008). The N_2 excess is the dominant product of denitrification, so analysis of such data with an appropriate model can yield an estimate of ϵ_{wcd} (Mariotti et al., 1981; Barford et al., 1999). In the context of the model presented here, the N_2 excess $\delta^{15}N$ has the advantage of not depending directly on the $\delta^{15}N$ of sinking material remineralized outside the suboxic zone. However, the measurement is analytically challenging, partially due to the large background of dissolved N_2 from equilibration with the atmosphere.

A fourth potential source of constraints is the oxygen isotopic composition of nitrate. Denitrification elevates nitrate $\delta^{15}N$ and $\delta^{18}O$ nearly equally (Granger et al., 2008). However, the $\delta^{15}N$ and $\delta^{18}O$ of nitrate respond differently to N cycling between nitrate and organic N through upwelling, nitrate assimilation, N sinking, and subsurface remineralization. While the $\delta^{15}N$ of the initial nitrate is roughly maintained by this cycle, the $\delta^{18}O$ of nitrate is reset to its “nitrification value” upon the return of N to the nitrate form. This N to O isotope distinction is clear in large ocean data sets from both the Pacific and the Atlantic (Rafter et al., 2013; Marconi et al., 2015). Thus, while ϵ_{wcd} may be overestimated due to oxalic remineralization on the relevant isopycnals, this should not be the case for $^{18}\epsilon_{wcd}$.

We have repeated our model experiments for the O isotopes of nitrate and compared them with the O isotope data from the same sample sets as used above. We find that the nitrate $\delta^{18}O$ data are roughly consistent with an $^{18}\epsilon_{wcd}$ of 25‰ but not consistent with an $^{18}\epsilon_{wcd}$ of 13‰ (Supplementary Fig. 4). Thus, one might take this result as ruling out the lower value for $^{18}\epsilon_{wcd}$. However, suboxic zone nitrate isotope data show variations in the $\delta^{18}O$ -to- $\delta^{15}N$ relationship that, along with other data, point to additional biogeochemical processing of nitrate in the suboxic zones that may raise the $\delta^{18}O$ above expectations from a given $^{18}\epsilon_{wcd}$ (Sigman et al., 2005; Casciotti and McIlvin, 2007; Casciotti, 2009; Buchwald and Casciotti, 2010; Casciotti and Buchwald, 2012; Casciotti et al., 2013). Nitrogen cycling within suboxic zones can either elevate the $\delta^{18}O$ of nitrate relative to its $\delta^{15}N$ or the opposite (Casciotti and Buchwald, 2012). Elevation of $\delta^{18}O$ relative to $\delta^{15}N$ occurs when net nitrate consumption by denitrification is more modest, as in the entire ETNP and everywhere but the core of the suboxic zone in the ETSP (Sigman et al., 2005; Casciotti and McIlvin, 2007; Casciotti et al., 2013). In contrast, elevation of $\delta^{15}N$ relative to $\delta^{18}O$ occurs under the highest degrees of nitrate consumption (in the core of the ETSP suboxic zone; Casciotti et al., 2013). In any case, with regard to the plausibility of a low ϵ_{wcd} (and thus a low $^{18}\epsilon_{wcd}$), the constraints provided by the $\delta^{18}O$ of nitrate in the ETNP suboxic zone are not yet clear.

5. CONCLUSIONS

Our model simulations and data comparisons show that the nitrate $\delta^{15}N$ observed in the denitrification zone of the ETNP could be the result of an isotope effect for water

column denitrification (ϵ_{wcd}) much lower than the value of $\sim 25\text{‰}$ that has been suggested by traditional Rayleigh model treatments of suboxic zone water column depth profile data. The ETNP data can be explained with an ϵ_{wcd} as low as $\sim 13\text{‰}$, a value suggested to be of potential physiological relevance by a recent culture study (Kritee et al., 2012). Specifically, we demonstrate how an overestimation of ϵ_{wcd} by the traditional Rayleigh treatment can result from aerobic respiration of sinking organic material within shallow to mid-depth water masses sourced from the Southern Ocean. The properties of these water masses would impact nutrient concentrations and nitrate $\delta^{15}N$ in the suboxic zone through lateral exchange along isopycnals. An estimate for the flux-weighted mean $\delta^{15}N$ of sinking N between the Southern Ocean and the Equatorial Pacific based on observational data suggests a mean sinking flux $\delta^{15}N$ of 8–10‰, consistent with a low ϵ_{wcd} of $\sim 13\text{‰}$. The canonical value of ϵ_{wcd} of 25‰ would require a lower mean sinking flux $\delta^{15}N$ of 3–4‰. However, while consistent with the observational $\delta^{15}N$ data investigated, the new mechanism we describe here cannot explain observed $\delta^{18}O$ of nitrate in suboxic zones. Moreover, this mechanism is unlikely to be the only process confounding the estimation of the water column isotope effect of denitrification. This mechanism is very likely to work in concert with others. These include the “mixing effect” and the oxidation of nitrite in the suboxic zone. The former is the regional cousin of the “dilution effect” acting on the global ocean (Deutsch et al., 2004) that is implicitly included in our model. The latter has been recently described by Casciotti et al. (2013) and is not addressed in this work. If an $\epsilon_{wcd} \sim 13\text{‰}$ is borne out, the N isotope budget of the ocean must be revisited. In particular, the lower ϵ_{wcd} would imply a lower rate of total denitrification, closer than previous estimates to the estimated rate of fixed N input to the ocean.

ACKNOWLEDGEMENTS

We thank Mathis P. Hain, Michael L. Bender, Bess B. Ward and Gerald H. Haug for the thoughtful input and intellectual support. A special thanks to all the nice people in the Sigman group at Princeton. Three anonymous reviewers and associate editor Silke Severmann greatly improved the manuscript. This work was supported by the US NSF through grant OCE-0960802 to D.M.S.

APPENDIX A. SUPPLEMENTARY DATA

Supplementary data associated with this article can be found, in the online version, at <http://dx.doi.org/10.1016/j.gca.2016.10.012>.

REFERENCES

- Alkhatib M., Lehmann M. F. and del Giorgio P. A. (2012) The nitrogen isotope effect of benthic remineralization–nitrification–denitrification coupling in an estuarine environment. *Biogeochemistry* **9**, 1633–1646.
- Altabet M. A. and Francois R. (1994) Sedimentary nitrogen isotopic ratio as a recorder for surface ocean nitrate utilization. *Global Biogeochem. Cycles* **8**(1), 103–116.

- Altabet M. A., Pilskaln C., Thunell R., Pride C., Sigman D. M., Chavez F. and Francois R. (1999) The nitrogen isotope biogeochemistry of sinking particles from the margin of the eastern North Pacific. *Deep-Sea Res. I* **46**, 655–679.
- Anderson L. (1995) On the hydrogen and oxygen content of marine phytoplankton. *Deep-Sea Res. I* **42**, 1675–1680.
- Barford C. C., Montoya J. P., Altabet M. A. and Mitchell R. (1999) Steady-state nitrogen isotope effects of N₂ and N₂O production in *Paracoccus denitrificans*. *Appl. Environ. Microbiol.* **65**, 989–994.
- Brandes J. A. and Devol A. H. (1997) Isotopic fractionation of oxygen and nitrogen in coastal marine sediments. *Geochim. Cosmochim. Acta* **61**(9), 1793–1801.
- Brandes J. A. and Devol A. H. (2002) A global marine fixed nitrogen isotopic budget: implications for Holocene nitrogen cycling. *Global Biogeochem. Cycles* **16**(4), 1120–1134.
- Brandes J. A., Devol A. H., Yoshinari T., Jayakumar D. A. and Naqvi S. W. A. (1998) Isotopic composition of nitrate in the central Arabian Sea and eastern tropical North Pacific: a tracer for mixing and nitrogen cycles. *Limnol. Oceanogr.* **43**(7), 1680–1689.
- Bristow L. A., Dalsgaard T., Tianio L., Mills D. B., Bertagnolli A. D., Wright J. J., Hallam S. J., Ulloa O., Canfield D. E., Revsbech N. P. and Thamdrup B. (2016) Ammonium and nitrite oxidation at nanomolar oxygen concentrations in oxygen minimum zone waters. *Proc. Natl. Acad. Sci. U.S.A.* **113**(38), 10601–10606.
- Brunner B., Contreras S., Lehmann M. F., Matantseva O., Rollog M., Kalvelage T., Klockgether G., Lavik G., Jetten M. S. M., Kartal B. and Kuypers M. M. M. (2013) Nitrogen isotope effects induced by anammox bacteria. *Proc. Natl. Acad. Sci. U.S.A.* **110**(47), 18994–18999.
- Buchwald C. and Casciotti K. L. (2010) Oxygen isotopic fractionation and exchange during bacterial nitrite oxidation. *Limnol. Oceanogr.* **55**, 1064–1074.
- Carpenter E., Harvey H., Fry B. and Capone D. (1997) Biogeochemical tracers of the marine cyanobacterium *Trichodesmium*. *Deep-Sea Res. I* **44**(1), 27–38.
- Casciotti K. L. (2009) Inverse kinetic isotope fractionation during bacterial nitrite oxidation. *Geochim. Cosmochim. Acta* **73**, 2061–2076.
- Casciotti K. L. and Buchwald C. (2012) Insights on the marine microbial nitrogen cycle from isotopic approaches to nitrification. *Front. Microbiol.* **3**(356), 1–14.
- Casciotti K. L. and McIlvin M. R. (2007) Isotopic analyses of nitrate and nitrite from reference mixtures and application to Eastern Tropical North Pacific waters. *Mar. Chem.* **107**, 184–201.
- Casciotti K. L., Trull T. W., Glover D. M. and Davies D. (2008) Constraints on nitrogen cycling at the sub-tropical North Pacific Station ALOHA from isotopic measurements of nitrate and particulate nitrogen. *Deep Sea Res. II* **55**, 1661–1672.
- Casciotti K. L., Buchwald C. and McIlvin M. (2013) Implications of nitrate and nitrite isotopic measurements for the mechanisms of nitrogen cycling in the Peru oxygen deficient zone. *Deep Sea Res. I: Oceanogr. Res. Pap.* **80**, 78–93.
- Codispoti L. A. and Christensen J. P. (1985) Nitrification, denitrification and nitrous oxide cycling in the eastern tropical South Pacific Ocean. *Mar. Chem.* **16**, 277–300.
- Deutsch C., Gruber N., Key R. M., Sarmiento J. L. and Ganaschaud A. (2001) Denitrification and N₂ fixation in the Pacific Ocean. *Global Biogeochem. Cycles* **15**(2), 483–506.
- Deutsch C., Sigman D., Thunell R. C., Meckler A. N. and Haug G. H. (2004) Isotopic constraints on glacial/interglacial changes in the oceanic nitrogen budget. *Global Biogeochem. Cycles* **18**, 1–24.
- Deutsch C., Sarmiento J. L., Sigman D. M., Gruber N. and Dunne J. P. (2007) Spatial coupling of nitrogen inputs and losses in the ocean. *Nature* **445**, 163–167.
- DeVries T., Deutsch C., Primeau F., Chang B. X. and Devol A. H. (2012) Global rates of water-column denitrification derived from nitrogen gas measurements. *Nat. Geosci.* **5**, 547–550.
- DeVries T., Deutsch C., Rafter P. A. and Primeau F. (2013) Marine denitrification rates determined from a global 3-dimensional inverse model. *Biogeosciences* **10**, 2481–2496.
- Eugster O. and Gruber N. (2012) A probabilistic estimate of global marine N-fixation and denitrification. *Global Biogeochem. Cycles* **26**(40), 1–15.
- Granger J., Sigman D. M., Lehmann M. F. and Tortell P. D. (2008) Nitrogen and oxygen isotope fractionation during dissimilatory nitrate reduction by denitrifying bacteria. *Limnol. Oceanogr.* **53**, 2533–2545.
- Granger J., Prokopenko M. G., Sigman D. M., Mordy C. W., Morse Z. M., Morales L. W., Sambrotto R. N. and Plessen B. (2011) Coupled nitrification-denitrification in sediment of the eastern Bering Sea shelf leads to ¹⁵N enrichment of fixed N in shelf waters. *J. Geophys. Res.* **116**, 1–18.
- Gruber N. (2004) The dynamics of the marine nitrogen cycle and its influence on atmospheric CO₂. In *Carbon Climate Interactions* (eds. T. Oguz and M. Follows). Kluwer Academic, Dordrecht.
- Hartin C. A., Fine R. A., Sloyan B. M., Talley L. D. and Happell J. (2011) Formation rates of subantarctic mode water and antarctic intermediate water in the Southeast Pacific. *Deep Sea Res. I* **58**, 524–534.
- Key R. M., Kozyr A., Sabine C. L., Lee K., Wanninkhof R., Bullister J., Feely R. A., Millero F., Mordy C. and Peng T. H. (2004) A global ocean carbon climatology: results from GLODAP. *Global Biogeochem. Cycles* **18**, 1–23.
- Kock A., Arevalo-Martinez D. L., Loscher C. R. and Bange H. W. (2016) Extreme N₂O accumulation in the coastal oxygen minimum zone off Peru. *Biogeosciences* **13**, 827–840.
- Kononov S. K., Fuchsman C. A., Belokopitov V. and Murray J. W. (2008) Modeling the distribution of nitrogen species and isotopes in the water column of the Black Sea. *Mar. Chem.* **111**, 106–124.
- Kritee K., Sigman D. M., Granger J., Ward B. B., Jayakumar A. and Deutsch C. (2012) Reduced isotope fractionation by denitrification under conditions relevant to the ocean. *Geochim. Cosmochim. Acta* **92**, 243–259.
- Lehmann M. F., Sigman D. M. and Berelson W. M. (2004) Coupling the N-15/N-14 and O-18/O-16 of nitrate as a constraint on benthic nitrogen cycling. *Mar. Chem.* **88**(1–2), 1–20.
- Lehmann M. F., Sigman D. M., McCorkle D. C., Granger J., Hoffmann S., Cane G. and Brunelle B. G. (2007) The distribution of nitrate ¹⁵N/¹⁴N in marine sediment sand the impact of benthic nitrogen loss on the isotopic composition of oceanic nitrate. *Geochim. Cosmochim. Acta* **71**, 5384–5404.
- Marconi D., Weigand M. A., Rafter P. A., McIlvin M. R., Forbes M., Casciotti K. L. and Sigman D. M. (2015) Nitrate isotope distributions on the US GEOTRACES North Atlantic cross-basin section: signals of polar nitrate sources and low latitude nitrogen cycling. *Mar. Chem.* **177**(1), 143–156.
- Mariotti A., Germon J. C., Hubert P., Kaiser P., Letolle R., Tardieux A. and Tardieux P. (1981) Experimental determinations of nitrogen kinetic isotope fractionation: some principles, illustration for the denitrification and nitrification processes. *Plant Soil* **62**, 413–430.
- Moore J. and Doney S. (2007) Iron availability limits the ocean nitrogen inventory stabilizing feedbacks between marine den-

- itrification and nitrogen fixation. *Global Biogeochem. Cycles* **21**, 1–12.
- Nikulin M. S. (2001) Loss function. In *Encyclopedia of Mathematics* (ed. M. Hazewinkel). Springer.
- Paulmier A., Kriest I. and Oschlies A. (2009) Stoichiometries of remineralisation and denitrification in global biogeochemical ocean models. *Biogeosciences* **6**, 923–935.
- Qu T. and Lindstrom E. J. (2004) Northward intrusion of Antarctic intermediate water in the Western Pacific. *J. Phys. Oceanogr.* **34**, 2104–2118.
- Rafter P. A., Sigman D. M., Charles C. D., Kaiser J. and Haug G. H. (2012) Subsurface tropical Pacific nitrogen isotopic composition of nitrate: biogeochemical signals and their transport. *Global Biogeochem. Cycles* **26**, 1–14.
- Rafter P. A., DiFiore P. J. and Sigman D. M. (2013) Coupled nitrate nitrogen and oxygen isotopes and organic matter remineralization in the Southern and Pacific Oceans. *J. Geophys. Res.: Oceans* **118**, 4781–4794.
- Redfield A. C., Ketchum B. H. and Richards F. A. (1963) The influence of organisms on the composition of sea-water. In *The Sea* (ed. M. Hill). Interscience, New York, pp. 26–77.
- Ren H., Sigman D. M., Meckler A. N., Plessen B., Robinson R. S., Rosenthal Y. and Haug G. H. (2009) Foraminiferal isotope evidence of reduced nitrogen fixation in the ice age Atlantic Ocean. *Science* **323**, 244–248.
- Revsbech N. P., Thamdrup B. and Dalsgaard T. (2011) Construction of STOX oxygen sensors and their application for determination of O₂ concentrations in oxygen minimum zones. *Methods Enzymol.* **486**, 325–341.
- Robinson R. S. et al. (2012) A review of nitrogen isotopic alteration in marine sediments. *Paleoceanography* **27**, 1–13.
- Ryabenko E., Kock A., Bange H. W., Altabet M. A. and Wallace D. W. R. (2012) Contrasting biogeochemistry of nitrogen in the Atlantic and Pacific oxygen minimum zones. *Biogeosciences* **9**, 203–215.
- Sarmiento J. L., Gruber N., Brzezinski M. A. and Dunne J. P. (2004) High latitude controls of the global nutrient and low latitude biological productivity. *Nature* **427**, 56–60.
- Sebilo M., Billen G., Grably M. and Mariotti A. (2003) Isotopic composition of nitrate-nitrogen as a marker of riparian and benthic denitrification at the scale of the whole Seine River system. *Biogeochemistry* **63**(1), 35–51.
- Sigman D. M., Casciotti K. L., Andreani M., Barford C., Galanter M. and Bohlke J. K. (2001) A bacterial method for the nitrogen isotopic analysis of nitrate in seawater and freshwater. *Anal. Chem.* **73**(17), 4145–4153.
- Sigman D. M., Robinson R., Knapp A. N., van Geen A., McCorkle D. C., Brandes J. A. and Thunell R. C. (2003) Distinguishing between water column and sedimentary denitrification in the Santa Barbara Basin using the stable isotopes of nitrate. *Geochem. Geophys. Geosyst.* **4**(5), 1040–1060.
- Sigman D. M., Granger J., DiFiore P., Lehmann M. F., van Geen A., Ho R. and Cane G. (2005) Coupled nitrogen and oxygen isotope measurements of nitrate along the eastern North Pacific margin. *Global Biogeochem. Cycles* **19**, 1–14.
- Sigman D. M., Karsh K. L. and Casciotti K. L. (2009a) *Ocean Process Tracers: Nitrogen Isotopes in the Ocean. Encyclopedia of Ocean Sciences*. Academic Press, New York, pp. 4138–4153.
- Sigman D. M., DiFiore P. J., Hain M. P., Deutsch C., Wang Y., Karl D. M., Knapp A. N., Lehmann M. F. and Pantoja S. (2009b) The dual isotopes of deep nitrate as a constraint on the cycle and budget of oceanic fixed nitrogen. *Deep-Sea Res. I* **56**, 1419–1439.
- Sigman D. M., DiFiore P. J., Hain M. P., Deutsch C. and Karl D. M. (2009c) Sinking organic matter spreads the nitrogen isotope signal of pelagic denitrification in the North Pacific. *Geophys. Res. Lett.* **36**, 1–5.
- Somes C. J., Oschlies A. and Schmittner A. (2013) Isotopic constraints on the pre-industrial oceanic nitrogen budget. *Biogeosciences* **10**(9), 5889–5910.
- Straub M., Sigman D. M., Ren H., Martinez-Garcia A., Meckler A. N., Hain M. P. and Haug G. H. (2013) Changes in North Atlantic nitrogen fixation controlled by ocean circulation. *Nature* **501**, 200–203.
- Tyrrell T. (1999) The relative influences of nitrogen and phosphorus on oceanic primary production. *Nature* **400**(6477), 525–531.
- Voss M., Dippner J. W. and Montoya J. P. (2001) Nitrogen isotope patterns in the oxygen-deficient waters of the eastern tropical North Pacific Ocean. *Deep-Sea Res. I* **48**, 1905–1921.
- Wald A. (1949) Statistical decision functions. *Ann. Math. Stat.* **20** (2), 165–205.

Associate editor: Silke Severmann